Physics Procedia

Volume 75, 2015, Pages 238–244

20th International Conference on Magnetism

Anisotropy, Magnetostriction and Converse Magnetoelectric effect in Dy substituted Ni Ferrite

Abhishek Majumder[1], Kodam Ugendar[1], Anoop Baby K. B.[1],Venkatarao Chunchu[1], R. A. Mondal[2] and G. Markandeyulu[1*]

[1] *Advanced Magnetic Materials Laboratory, Department of Physics, Indian Institute of Technology Madras, Chennai 600 036 India*

[2] *Microwave Laboratory, Department of Physics, Indian Institute of Technology Madras, Chennai 600 036 India [Presently at: Department of Physics, Hindustan University, Chennai 603103 India]*

mark@iitm.ac.in

Abstract

$NiFe_{2-x}Dy_xO_4$ (x = 0, 0.1) compounds were prepared by solid state reaction. Room temperature X-ray diffraction confirmed the formation of the compounds in cubic inverse spinel phase with the space group $Fd\bar{3}m$. Increments in the lattice constant were observed upon partial substitution of Fe^{3+} by Dy^{3+}. While both magnetization and cubic magnetocrystalline anisotropy (K_1) decreased with increasing temperature, with Dy^{3+} substitution, at any given temperature the magnetization decreased and K_1 increased. A quantitative observation of direct magnetoelectric (DME) effect and qualitative observation of converse magnetoelectric (CME) effect in $NiFe_{1.9}Dy_{0.1}O_4$ compound, describe its multiferroic nature.

Keywords: Magnetoelectric effect, Ferrites, Converse magnetoelectric effect, Anisotropy

1 Introduction

Multiferroic materials [1] have been attracting the attention of researchers and technologists alike, due to the interesting interplay between the various physical properties as well as their applicability in transducers, sensors, actuators, filters, non-volatile memories etc., [2] [3] [4]. The unique feature of multiferroic materials is the magnetoelectric (ME) effect, a coupling between magnetic and ferroelectric orders, which is of great importance for memory, logic devices and has potential applications for next generation devices [1] [5]. Direct magnetoelectric (DME) effect and converse magnetoelectric (CME) effects are two types of classifications in ME effect [6].

* Corresponding author

Selection and peer-review under responsibility of the Scientific Programme Committee of ICM 2015

doi:10.1016/j.phpro.2015.12.029

Nickel ferrite (NFO) possesses high permeability, low coercivity, reasonable magnetostriction and high resistance that render it useful in high frequency applications [7] [8]. It is known that in NFO, the tetrahedral (A) sites are occupied by Fe^{3+} ions and the octahedral (B) sites are occupied by Ni^{2+} and Fe^{3+} ions in equal proportions [7]. Partial substitution of Fe^{3+} by rare-earth (R^{3+}) ion in the B-site has been reported to lead to structural distortion [9] that induces strains and significantly modifies the electrical and dielectric properties [10] [11].

Dinesh *et.al* have reported that (65PIN – 35PT)-NFO laminate composite shows self-biased DME coefficient of 8 V/cm-Oe and a CME coefficient of 5 mG-cm/V [12]. Many single phase ferrites with perovskite structure could also exhibit magnetoelectric effect [5] [13] [14] [15] [16]**.** Shuiyuan Chena *et.al* have investigated multiferroic properties of $Bi_{1-x}Ca_xFeO_3$ and reported a converse magnetoelectric coefficient of 6.48×10^{-11} s/m [15]. Dascalu *et.al* have reported decreased magnetization and magnetostriction when Fe is partially substituted by rare earth in $CoFe_2O_4$ [17] From our lab, Kamala Bharati *et.al* [18] have observed ferroelectricity and magnetocapacitance in Gd and Nd substituted Nickel ferrite and have also reported increased magnetocapacitance and magnetic field dependent ferroelectric loop in $NiFe_{1.925}Dy_{0.075}O_4$ [10]. In $NiFe_{1.925}Sm_{0.075}O_4$ thin films coated on PZT, linear magnetoelectric coefficient of 407 mV/cm-Oe at 500 Oe has been reported [19]. In this paper, anisotropy, DME and CME in $NiFe_{1.9}Dy_{0.1}O_4$ are reported.

2 Experimental Details

Polycrystalline compounds $NiFe_{2-x}Dy_xO_4$ (x = 0, 0.1) were prepared, starting from NiO (99.96% pure) Fe_2O_3 and Dy_2O_3 (99.99% pure), by the solid state reaction method. Powders of the starting materials were ground in an agate mortar and pestle for three hours and the mixtures were kept in a resistive heating furnace and heat treated in air at 1240 ^{0}C for 12 h. The formation of the samples in inverse spinel phase was confirmed by powder X-ray diffraction (XRD) technique using a PANalytical (X'pert PRO) x-ray diffractometer employing Cu K_α radiation. Magnetization measurements were carried out using a Quantum design MPMS 3 SQUID based VSM. Magnetostriction measurements were carried out, employing a commercial strain gauge (of resistance 120 Ω) with a gauge factor of 2 ± 0.03 and using a Model 3800 Wide Range Strain Indicator. The instrument was calibrated with a standard 120 Ω resistor before measurements. For the dielectric, magnetic, magnetoelectric and converse magnetoelectric measurements, the powders were made into pellets which were then sintered at 1240 ^{0}C in air for 12 h.

3 Results and discussion

Figure 1 shows the XRD patterns of $NiFe_{2-x}Dy_xO_4$ (x = 0, 0.1) respectively along with the calculated parameters after Rietveld refinement. The weighted refined parameter (ω_{rp}), χ^2, lattice constant (a), bond angles and bond length values of the fitting are given in Table 1. Both the compounds were found to crystallize in the cubic inverse spinel phase with a small amount of $DyFeO_3$ phase in the latter. In $NiFe_{1.9}Dy_{0.1}O_4$, the weight fractions of the inverse spinel phase and $DyFeO_3$ are 0.964 and 0.036 respectively. The lattice constant of $NiFe_2O_4$ was found to be 8.3415 Å which is in good agreement with the reported value (8.34 Å [7]). An increment in the lattice constant value from 8.3415 Å to 8.3460 Å was observed in the case of $NiFe_{1:9}Dy_{0.1}O_4$, attributed to substitution of Fe^{3+} ion by the larger Dy^{3+} ion in the octahedral (B) site. From Table 1, it is clear that, the changes in the B-site bond angles, Fe^{3+} - O^{2-} - Fe^{3+}/Dy^{3+} and the B-site bond lengths O^{2-} - Fe^{3+}/Dy^{3+} in $NiFe_{1:9}Dy_{0.1}O_4$ (compared to the values in $NiFe_2O_4$) cause a small distortion in the lattice.

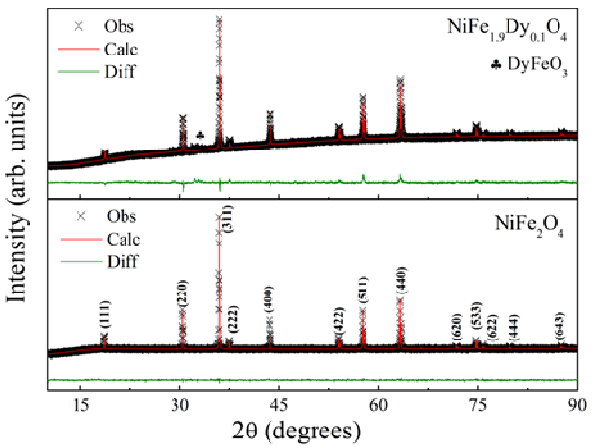

Figure 1: Rietveld refined XRD patterns of $NiFe_{2-x}Dy_xO_4$ (x = 0, 0.1)

The dielectric measurements were carried out on the $NiFe_{1.9}Dy_{0.1}O_4$ pellet and the results are shown in Figure 2. The permittivity is seen to decrease with frequency as in the nickel ferrite [10]. At high frequencies, the sample is seen to exhibit very low permittivity values, which can be explained on the basis of the Maxwell–Wagner theory of interfacial polarization and the Koops phenomenological model [20]. It can be seen that the value of ε' increases rapidly with increase in temperature at low frequencies, which can be attributed to the temperature dependent interfacial and dipolar polarizations.

The resistivity measurement indicates that the ac resistivity of the $NiFe_{1.9}Dy_{0.1}O_4$ sample decreases with increase in frequency (Figure 3), which can be explained by the Verwey-de Boer hopping mechanism of charge carriers [20]. As the frequency of applied electric field increases, the frequency of electron hopping between Fe^{2+} and Fe^{3+} ions in the octahedral sites also increases which in turn decreases the resistivity of the material. Also, the resistivity was found to decrease with temperature due to the presence of thermally activated charge carriers.

Parameter		**$NiFe_2O_4$**	**$NiFe_{1.9}Dy_{0.1}O_4$**
Lattice constant (Å)		8.3415	8.3460
χ^2		1	1.714
ω_{rp}		1.67	1.98
Bond length (Å)	O^{2-} - Fe^{3+} (B)	2.031	2.067
	O^{2-} - Fe^{3+} (A)	1.902	1.840
Bond angle (Degrees)	Fe^{3+} (A) - O^{2-} - Fe^{3+}/Dy^{3+} (B)	123.0	124.5
	Ni^{2+} - O^{2-} - Ni^{2+}	93.0	91.0
	O^{2-} - Fe^{3+} (A) - O^{2-}	109.4	109.4
	O^{2-} - Fe^{3+} (B) - O^{2-}	86.9	91.0

Table 1: Structural parameter of $NiFe_{2-x}Dy_xO_4$ (x = 0, 0.1)

Magnetization was measured at 20 K and 50 K to 300 K in steps of 50 K, using a VSM employing a SQUID based detector. Figure 4 shows the magnetization curves of $NiFe_{2-x}Dy_xO_4$ (x = 0, 0.1). Partial substitution of Fe^{3+} by Dy^{3+} is seen to cause the M_s at 20 K, to decreases from 56.39 emu/g to 52 emu/g. The magnetization data at fields above 9 kOe were fit to the Law of Approach to Saturation (LAS) for cubic anisotropy systems, approximated by [7] [21]

$$|M(H)| = M_s - \frac{8K_1^2}{105\mu_0 M_s H^2} + \kappa H \qquad (1)$$

where K_1 is the first order cubic magnetocrystalline anisotropy constant. The numerical coefficient 8/105 has been obtained for a polycrystalline material. The last term κH represents forced magnetization due to the increase of saturation magnetization in high fields and κ represents paramagnetic susceptibility which was neglected in the present case as there are no paramagnetic impurities.

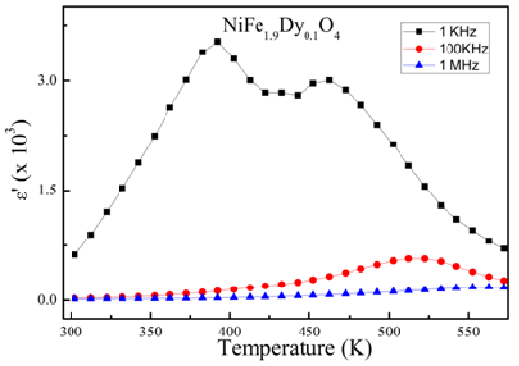

Figure 2 Plot of permittivity *vs* temperature of $NiFe_{1.9}Dy_{0.1}O_4$ for different frequencies

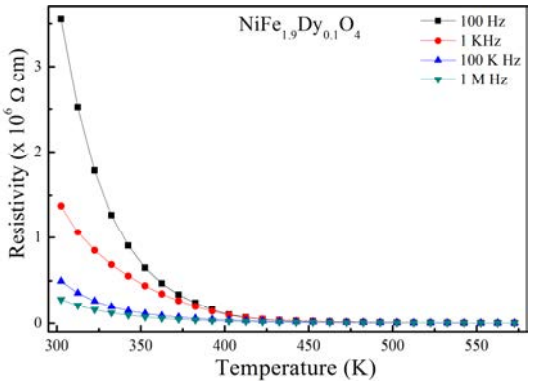

Figure 3: Plot of resistivity *vs* temperature of $NiFe_{1.9}Dy_{0.1}O_4$ for different frequencies

Inset of Figure 5 shows the values of K_1 and M_s of $NiFe_{1:9}Dy_{0.1}O_4$. The value of K_1 of $NiFe_{1:9}Dy_{0.1}O_4$ at 20 K is 92 kJ/m^3, more than that of $NiFe_2O_4$ (42 kJ/m^3). The anisotropy is thus seen to increase with Dy substitution. The observed increase in K_1 is attributed to the large negative anisotropy value of Dy [7]. Magnetostriction data on $NiFe_{2-x}Dy_xO_4$ (x = 0, 0.1) at room temperature is shown in Figure 5. The measurements were performed by the strain gauge (of resistance 120 Ω) method. The saturation magnetostriction (λ_S) values are found to be -32 x10^{-6} and -35 x 10^{-6} respectively. The value of λ_S for $NiFe_2O_4$ is in good agreement with the reported value [10] [20]. For $NiFe_{1:9}Dy_{0.1}O_4$ the slope of the magnetostriction curve at low field is found to be larger compared to that of $NiFe_2O_4$, which can be attributed to the increase in the anisotropy with the substitution of Dy^{3+}.

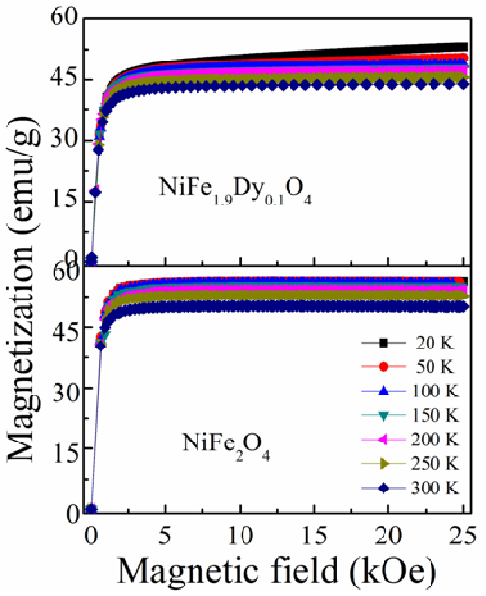

Figure 4: Magnetization curves of $NiFe_{2-x}Dy_xO_4$ (x = 0, 0.1) at different temperatures

The DME coefficient of $NiFe_{1:9}Dy_{0.1}O_4$ was measured at room temperature using a commercial set up manufactured by Marine India. The voltage developed across the thickness of the pellet was measured, by the application of a static magnetic bias field up to 1.5 kOe. Lock-in method was employed for which, an alternating magnetic field (10 Oe at 850 Hz) was applied using a Helmholtz coil arrangement. A circular pellet, which were electrically poled along its axis in an electric field of 0.4 kV/cm for 24 hrs and then magnetically poled perpendicular to its axis by a field of strength of 0.8 T for 2 hrs, were used for determining the DME coefficient. The induced voltage (V) was measured along the axis of the pellet. The ME coefficient was calculated as α_{ME} = V / (t • H_{ac}) where t is the thickness of the pellet. Figure 6 shows the plot of α_{ME} *vs* magnetic field. The value of α_{ME} increases with the DC magnetic field, attains a maximum value of 32.7 mV/cm-Oe at 473 Oe and then decreases with further increase of the field. Kamala Bharati *et.al* have reported increased magneto-capacitance and magnetic field dependent

ferroelectric loop in $NiFe_{1.925}Dy_{0.075}O_4$ [10]. The observed α_{ME} is due to the breakdown of centrosymmetry of the octahedral site, which leads to ferroelectricity and hence multiferroic properties in the investigated compounds [1] [5].

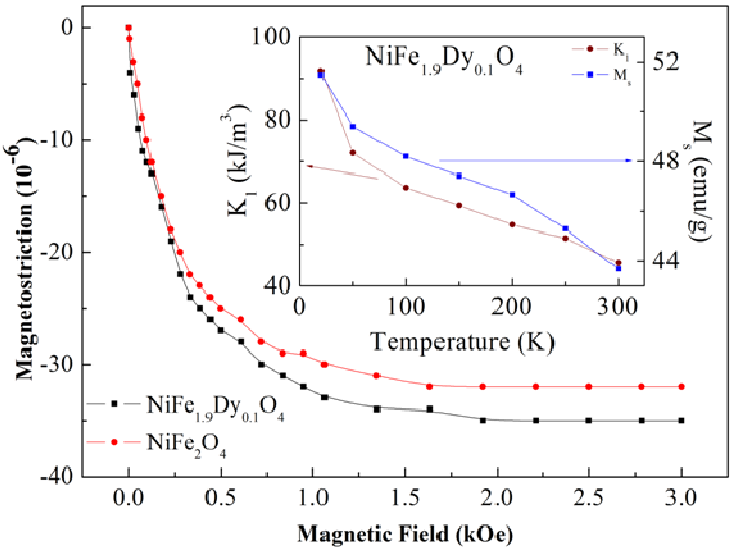

Figure 5: Room temperature magnetostriction of $NiFe_{2-x}Dy_xO_4$ (x = 0, 0.1). Inset: Temperature dependence of M_s and K_1 of $NiFe_{2-x}Dy_xO_4$ (x = 0, 0.1)

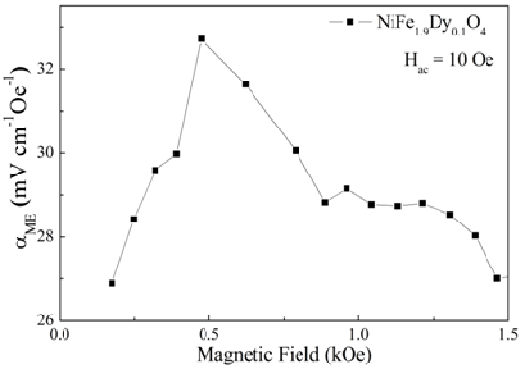

Figure 6: Plot of α_{ME} *vs* magnetic field at room temperature $NiFe_{1.9}Dy_{0.1}O_4$

The electrically poled pellet was used for CME studies. CME was observed by measuring the change in magnetoimpedance (MI) of a soft ferromagnetic ribbon upon the application of an external magnetic field. The soft magnetic ribbon was placed at a distance of 1 mm over the circular pellet in such a way that the axis of the ribbon coincided with the diameter (10 mm) of the pellet. The soft magnetic ribbon was connected to a HP4192A impedance analyzer and the impedance of the ribbon was measured both with and without the presence of the pellet in its vicinity, in the frequency range 0.5 MHz - 13 MHz. The percentage change in the impedance of the ribbon was calculated and compared with the MI data of the same ribbon in the above mentioned frequency range, which was measured earlier under an applied magnetic field ranging from -100 Oe to +100 Oe. The impedance of the soft magnetic ribbon was measured by changing the frequency from 0.5 MHz to 13 MHz. The frequency at which the magnetoimpedance of the ribbon was the largest (28%) was 5 MHz. The magnetic field developed due to poled $NiFe_{1:9}Dy_{0.1}O_4$ was determined as 0.535 Oe (42.8 A/m). This is an interesting observation in a single compound and may pave way for CME based transducers.

4 Conclusions

$NiFe_{2-x}Dy_xO_4$ (x = 0, 0.1) compounds crystallize in the cubic inverse spinel phase and an increase in lattice constant with Dy^{3+} content as confirmed by XRD patterns. Partial substitution of Fe^{3+} ions by Dy^{3+} ions, leads to a decrease in the magnetization and increase in K_1. Temperature dependent M-H data reveals that for both the compounds, the saturation magnetization and K_1 values decreased with increasing temperature. Linear DME coefficient of 32.7mV/cm-Oe and also a conspicuous and qualitative CME were observed in the $NiFe_{1.9}Dy_{0.1}O_4$ compound.

References

[1] M. Fiebig, "Revival of the magnetoelectric effect," *J. Phys. D,* vol. 38, pp. R123 - R152, 2005.

[2] C.-W. Nan and D. Clarke, "Effective properties of ferroelectrici and/or ferromagnetic composites: a unique approach and its application," *J. Am. Ceram. Soc.,* vol. 80, p. 1333, 1997.

[3] L. Mitoseriu, V. Buscaglia, M. Viviani, M. Buscaglia, I. Pallecchi, C. Harnagea, A. Testino, V. Trefiletti and P. Nanni, "BaTiO3-(Ni0.5Zn0.5)Fe2O4 ceramic composites with ferroelectric and magnetic properties," *J. Eur. Ceram. Soc.,* vol. 27, pp. 4379-4382, 2007.

[4] N. Fujimura, T. Ishida, T. Yoshimura and T. Ito, "Epitaxially grown YMnO3 film: new candidate for nonvolatile memory devices," *Appl. Phys. Lett.,* vol. 69, pp. 1011 - 1013, 1996.

[5] W. Eerenstein, N. Mathur and J. Scott, "Mutiferrioc and magnetoelectric materials," *Nature,* vol. 442, pp. 759-765, 2006.

[6] W. Eerenstein, M. Wiora, J. Prieto, J. Scott and N. Mathur, "Giant sharp and persistent converse magnetoelectric effects in multiferroic epitaxial heterostructures," *Nat. Mater.,* vol. 6, pp. 348-351, 2007.

[7] S. Chikazumi, Physics of Ferromagnetism, New York: Oxford University Press, 1997.

[8] U. Ozgur, Y. Alivov and H. Morkoc, "Microwave ferrites, part 1: fundamental properties," *J. Mater. Sco. Mater. Electron.,* vol. 20, pp. 799-834, 2009.

[9] N. Rezlescu and E. Rezlescu, "The Influence of Fe substitutions by R ions in a Ni-Zn ferrite," *Solid State Commun.,* vol. 88, pp. 139-141, 1993.

[10] K. Kamala Bharathi, K. Balamurugan, P. Santhosh, M. Pattabiraman and G. Markandeyulu, "Magnetocapacitance in Dy-doped Ni ferrite," *Phys. Rev. B,* vol. 77, p. 172401, 2008.

[11] E. Schloemann, "Advances in ferrite microwave materials and devices," *J. Magn.Magn. Mater.,* vol. 209, pp. 15-20, 2000.

[12] S. Dinesh Kumar, G. Ramesh and V. Subramanian, "Enhanced sef-biased direct and converse magnetoelectric effect in Pb(In1/2Nd1/2)O3-PbTiO3/NiFe2O4 bi-layer laminate composite," *J. Mater. Sco.: Mater. Electron.,* vol. 26, pp. 2682-2687, 2015.

[13] Y. Tokunaga, S. Iguchi, T. Arima and Y. Tokura, "Magnetic field induced ferroelectric state in DyFeO3," *Physical Review Letters* , vol. 101, p. 097205, 2008.

[14] C. Ederer and N. A. Spaldin, "Weak ferromagnetism and magnetoelectric coupling in bismuth ferrite," *Phy. Rev. B,* vol. 71, p. 060401 (R), 2005.

[15] S. Chena, L. Wang, H. Xuan, Y. Zheng, D. Wang, J. Wu, Y. Du and Z. Huang, "Multiferroic properties and converse magnetoelectric effect in Bi1−xCaxFeO3 ceramics," *Journal of Alloys and Compounds,* vol. 506, pp. 537-540, 2010.

[16] F. Sugawara, S. Iiida, S. Y. and A. S., "Magnetic properties and crystal distortions of Bi MnO3 and BiCrO3," *J. Phys. Soc. Jpn*, vol. 25, pp. 1553-1558, 1968.

[17] G. Dascalu, T.Popescu, M.Feder and O.F.Caltun, "Structural, electric and magnetic properties of CoFe1.8RE0.2O4 (RE Dy, Gd,La) bulk materials," *Journal of Magnetism and Magnetic Materials*, vol. 333, p. 69–74, 2013.

[18] K. Kamala Bharathi, J. Arout Chelvane and G. Markandeyulu, "Magnetoelectric properties of Gd and Nd- doped nickel ferrite," *J. Magn.Magn. Mater.*, vol. 321, pp. 3677-3680, 2009.

[19] K. Kamala Bharathi, S. Dwevedi, S. Venkatesh and G. Markandeyulu, "Structural, magnetic and magnetoelectric properties of NiO.Fe2O3 and NiO.Fe1.925Sm0.075O3," *J. Appl. Phys.*, vol. 107, p. 09D915, 2010.

[20] H. B. Callen and E. Callen, "The present status of the temperature dependence of magnetocrystalline anisotropy and the l(l+1)/2 power law," *J. Phys. Chem. Solids.*, vol. 27, pp. 1271-1285, 1966.

[21] P. Graves, C. Johnston and J. Campaniello, "Raman Scattering in spinel strcture ferrites," *Mater. Res. Bull.*,, vol. 23, pp. 1651-1660, 1988.

[22] V. Ivanov, M. Abrashev, M. Iliev, M. M. Gospodinov, J. Meen and M. Aroyo, "Short-range B-site ordering in the inverse spinel ferrite NiFe2O4," *Phys. Rev. B.*, vol. 82, p. 024101, 2010.

[23] J. Jacob and M. Abdul Khadar, "Investigation of mixed spinel structure of nanostrctured nickel ferrite," *J. Appl. Phys.*, vol. 107, p. 114310, 2010.

[24] J. Kreisel, G. Lucazeau and H. Vincent, "Raman Spectra and Vibrational Analysis of BaFe12O19 Hexagonal Ferrite," *J. Solid. State. Chem.*, vol. 137, pp. 127-137, 1998.

[25] J. Smith and H. P. J. Wijn, Ferrites, Philips Technical Library, Eindhoven, The Netherlands, 1965.

[26] Z. H. Zhou, J. M. Xue, J. Wang, H. S. O. Chan and T. Yu, "NiFe2O4 nanoparticles formed in situ in silica matrix by mechanical activation," *J. Appl. Phys.*, vol. 91, pp. 6015-6020, 2002.